Interferogram Filtering Using Gaussians Scale Mixtures In Steerable Wavelet Domain

Gh.S.El-Taweel g.sami@scuegypt.edu.eg
Faculty of Computers and Informatics / C.S. Dep.
Suez Canal University
Ismailia, Egypt

Ashraf. K. Helmy akhelmy@narss.sci.eg
National Authority for Remote Sensing
and Space Sciences,
Cairo, Egypt

Abstract

An interferogram filtering is presented in this paper. The main concern of the proposed scheme is to lower the residues count mean while preserving the location and jump height of the lines of phase discontinuity.
The proposed method uses Steerable wavelet decomposition. At each scale, a noise covariance matrix is estimated for the neighborhood of each pixel using an interferogram power spectral density. The estimated covariance is then used to produce a maximum a-posteriori estimate of the noise-free value of the pixel. After the image has been "de-noised" at each scale-level, it is then reconstructed.
Based on Portilla et. al., neighborhoods of coefficients at adjacent positions and scales are modeled as the product of two independent random variables, the Bayesian least squares estimate of each coefficient reduces to a weighted average of the local linear estimates over all possible values of the hidden multiplier variable. The performance of this method substantially has the advantages of reducing number of residuals without affecting line of height discontinuity.

Keywords: Radar Imaging, Phase Unwrapping, Interferogram, Gaussian scale mixtures

1. INTRODUCTION

Synthetic aperture radar (SAR) enables imaging of the ground by processing microwave backscattering data collected along the flight path of an airborne or space borne platform. This results in high-resolution images of the local complex reflectivity of the ground. For the SAR images obtained from slightly different flight paths, the complex-valued pixels of one image are multiplied with the co-registered complex conjugate pixels of the other, the phase of the resulting product image constitutes a SAR interferogram. The significance of this phase image is that it contains information on terrain height. With proper processing, it yields a so-called digital elevation model (DEM) which represents the topography of the terrain. Other significant of using phase image is to measure land subsidence, snow motion, monitoring sand dunes movements, and many others.

The SAR interferogram presents two main features preventing its direct use. The first one is that the phase is wrapped within the interval (-π, π), due to the periodic nature of the phase signal. In order to obtain the absolute phase, and therefore, to obtain the height information, it

is necessary to unwrap the phase signal [1]. From the other side, the interferometric phase signal is corrupted by noise. This noise, on a first stage, will affect the unwrapping process as it induces phase residues, which make the unwrapping process difficult. On a second stage, the own noise degrades the derived height information. In order to overcome these problems it is necessary to introduce a phase filtering process before phase unwrapping. This filtering process can be also thought as an estimation process.

The key computational problem in obtaining the DEM lies in the fact that the measured phase differences are undetermined within multiples of 2π. They are given as a wrapped phase field of principal values with range from -π to π. It is necessary to perform a 2-D phase unwrapping operation, which removes phase jumps between neighboring pixels larger than π by adding or subtracting multiples of 2π so that the resulting distribution can be considered as samples of an underlying smooth function. This is a noise-sensitive problem and subject of recent research [2]. The 2-D phase unwrapping problem can be stated as follows:

$$\psi(n_1,n_2) = \quad Arg\{e^{i[\phi(n_1 n_2+noise]}\} \qquad (1)$$

where ψ is the noisy wrapped interferogram, ϕ are samples of a smooth phase surface, and |Arg(.)| ≤ π is determination of an estimate ϕ from ψ. A major challenge of 2-D phase unwrapping comes from the fact that the noise in (1) due to, temporal de-correlation introduces local inconsistencies of the data referred to as residues. Any phase unwrapping algorithm is sensitive to the presence of residues that make contour integrations path-dependent.

Many interferogram filtering are introduced. Lee et. al. demonstrated that the interferometric phase noise can be modeled as an additive noise [3]. Other algorithm is based on a new interferometric phase noise model in the complex plane [2]. Some estimate the InSAR phase within a local estimation window based on the InSAR sample statistics [4, 5]. In general it can be stated that filtering process is mandatory as it not only reduces the error probability in subsequent phase unwrapping but also increases processing speed considerably [3].

This paper is a modification version of Portilla et. al. where local residual removal solution based on Baysian least square estimator is used. A model for neighborhoods of oriented pyramid coefficients based on Gaussian scale mixture is used and noise covariance matrix is estimated for the neighborhood of each pixel using an interferogram power spectral density via different sets of window shapes. We assume based on [6, 7] that the amplitude of coefficients of similar position, orientation and scaled are highly correlated. These higher order dependencies may be modeled by augmenting a factor for local dependences (Gaussian) with random variables that govern the parameters (variance). The remainder of the paper is organized as follows: section 2 focus on the interferomeric residual model, section 3 describe a brief introduction to steerable pyramid wavelet transform, section 4 depict the interferogram probability model, section 5 emphasis the proposed filtering process, section 5 shows the experiment result, and section 6 represents the conclusion.

2. INTERFEROMETRIC RESIDUAL MODEL

The interferometric phase is due to the interaction between two SAR images. The statistical behavior of the interferometric phase depends on this interaction. The interferometric coherence is the amplitude of the correlation coefficient between the two complex SAR images:

$$\rho = \frac{E\{I_1 \ I_2^*\}}{\sqrt{\{|I_1|^2\}E\{|I_2|^2\}}} |\rho| \ell^{j\phi} \qquad (2)$$

Where I_1 and I_2 represent the two SAR images, ρ is the coherence and ϕ_x is the corresponding interferometric phase. The interferometric phase has been completely

characterized in the real domain. For Gaussian scattering model and distributed scatterers, the interferometric phase follows the following distribution [1].

$$P_{\phi}(\phi)=\frac{\Gamma(n+\frac{1}{2})(1-|\rho|^2)^n\beta}{2\sqrt{\pi}\Gamma(n)(1-\beta^2)^{n+1/2}}+\frac{(1-|\rho|^2)^n}{2\pi}{}_2F_1(n,1;1/2;\beta^2) \quad (3)$$

Where $\beta=|\rho|-\cos(\phi-\theta)$, 2F1 represents the Gauss hyper-geometric functions and n is the number of looks. The probability density function (pdf) eq. (3) is symmetric (mod 2π) about its mode, which occurs at ϕ. Based on the distribution of the interferometric phase eq. (2), [3] demonstrated that the interferometric phase noise can be modeled as an additive Gaussian noise [8, 9]

$$\phi_z = \phi_x + v \quad (4)$$

Where ϕ_z is the measured interferometric phase, ϕ_x is the real interferometric phase and v represents the noise with the distribution listed in eq. (3). The measured phase ϕ_z can be encoded in the complex plane as a point in the unit circle:

$$e^{j\phi_z} = \cos(\phi_z) + j\sin(\phi_z) \quad (5)$$

Using the distribution (3) together with the properties of the trigonometric functions, the real and imaginary parts of (5) can be modeled as [9].

$$\cos(\phi_z) = Nc\cos(\phi_x) + v_c \quad (6)$$

$$\sin(\phi_z) = Nc\sin(\phi_x) + v_s \quad (7)$$

Based on (2), it can be demonstrated that the value of Nc, for n = 1, is:

$$N_c=\frac{\pi}{4}|\rho|_2F_1(1/2,1/2;2;|\rho|^2) \quad (8)$$

As equations (6), (7), and (8) show, N_c only depends on ρ. The terms vc and vs can be considered as noise terms, as their means are zero. These noise terms depend on the interferometric phase ϕ_x. This dependence does not affect the mean, which is zero, but only the standard deviation [9]. The dependence with the interferometric phase Φ_x can be neglected, and then, the variance of the noise terms can be approximated by the function:

$$\sigma_{v_c}^2=\sigma_{v_s}^2=\frac{1}{2}\left(1-|\rho^{0.68}|\right) \quad (9)$$

Eq's (6) and (7) can be seen respectively as a noise model for the real and imaginary parts of the interferometric phase in the complex plane. In each case, the signals to recover are $\cos(\phi_x)$ and $\sin(\phi_x)$. These signals are multiplied by N_c. As shown before, this parameter behaves in the same way as the coherence ρ does, so instead assuming it as a noise parameter, it can be considered as a useful parameter to recover. It was demonstrated that Nc can be employed to estimate the coherence ρ [9]. The main feature of this way to estimate the coherence is that the coherence information can be estimated with high spatial resolution.

3. STEERABLE PYRAMID

The Steerable Pyramid is a linear multi-scale, multi-orientation image decomposition that provides a useful front-end for image-processing and computer vision applications. It was developed in order to overcome the limitations of orthogonal separable wavelet decompositions that were becoming popular for image processing (specifically, those representations are heavily aliased, and do not represent oblique orientations well). Once the orthogonality constraint is dropped, it makes sense to completely reconsider the filter design

problem (as opposed to just re-using orthogonal wavelet filters in a redundant representation, as is done in cycle-spinning or undecimated wavelet transforms!). Detailed information may be found in the references listed below.

The basis functions of the steerable pyramid are directional derivative operators that come in different sizes and orientations. An example decomposition of an image of a white disk on a black background is shown to the right. This particular steerable pyramid contains 4 orientation sub-bands, at 2 scales. The number of orientations may be adjusted by changing the derivative order (for example, first derivatives yield two orientations). The smallest sub-band is the residual low-pass information. The residual high-pass sub-band is not shown.

Figure (1) shows the block diagram for the decomposition (both analysis and synthesis). Initially, the image is separated into low and high-pass sub-bands, using filters L_0 and H_0. The low-pass sub-band is then divided into a set of oriented band-pass sub-bands and a low pass sub-band. This lower pass sub-band is sub-sampled by a factor of 2 in the X and Y directions. The recursive (pyramid) construction of a pyramid is achieved by inserting a copy of the shaded portion of the diagram at the location of the solid circle (i.e., the low-pass branch) [10].

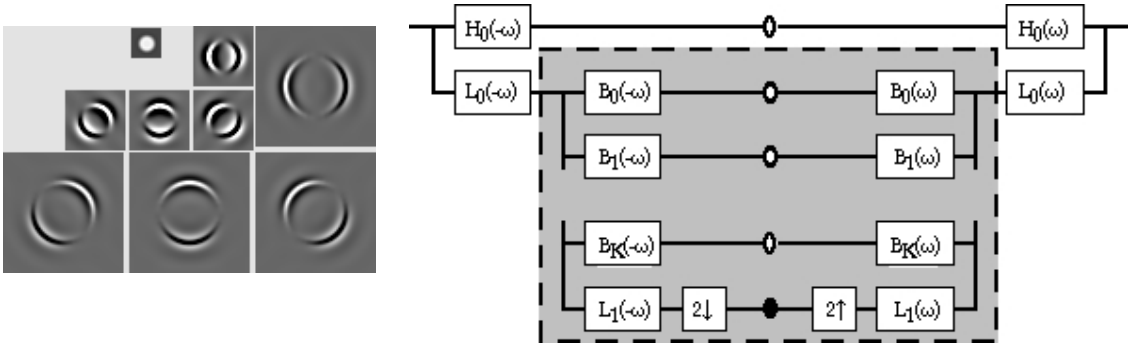

Figure: (1) Block diagram for Steerable Pyramid decomposition (analysis and synthesis).

4. INTERFEROGRAM PROBABILITY MODEL

Multiscale representations provide a useful front-end for representing the structures of 2-D signals. But they are critically sampled (the number of coefficients is equal to the number of image pixels), and this constraint leads to disturbing visual artifacts (i.e., “aliasing” or “ringing”). A widely followed solution to this problem is to use basis functions designed for orthogonal or biorthogonal systems, to reduce or eliminate the decimation of the subbands [11]. Once the constraint of critical sampling has been dropped, there is no need to limit oneself to these basis functions. Significant improvement comes from the use of representations with a higher degree of redundancy, as well as increased selectivity in orientation [12]. For the current paper, we have used a particular variant of an over complete tight frame representation known as a steerable pyramid [13]. The basis functions of this multiscale linear decomposition are spatially localized, oriented, and span roughly one octave in bandwidth. They are polar-separable in the Fourier domain, and are related by translation, dilation, and rotation.

4.1 Gaussian Scale Mixtures

Let an interferogram is decomposed into oriented subbands at multiple scales, and Let xcs,o(n,m) the coefficient corresponding to a linear basis function at scale (s) , orientation (o) , centered at spatial location 2sn, 2sm . We denote as xs,o(n,m) a neighborhood of coefficients clustered around this reference coefficient . in our case the neighborhood include coefficients from three subbands at adjacent scale (i.e., corresponding to basis functions at nearby scales and orientations), as well as from the same subband. Thus taking advantage of the strong statistical coupling observed through scale in multiscale representations.

Lee et. al. proposed that the residuals are characterized with an additive model [3]. We assume the coefficients within each local neighborhood around a reference coefficient of a pyramid subband are characterized by a Gaussian scale mixture (GSM) model. Formally, a random vector is a Gaussian scale mixture if and only if it can be expressed as the product of a zero-mean Gaussian vector (u) and an independent positive scalar random variable ($\sqrt{z}$)

$$X \equiv u * \sqrt{z} \qquad (10)$$

the variable z is known as the multiplier. The vector x is thus an infinite mixture of Gaussian vectors, whose density is determined by the covariance matrix Cu of vector u and the mixing density $p_z(z)$, and ($\equiv$) mean equal in distribution.

4. 2 Modeling Wavelet Coefficients

In order to construct model for interferogram, one must specify both the neighborhood structure of the coefficients, and the distribution of the multipliers. Regardless to the neighborhood structure of the coefficients, the window selected should be aligned along fringes to include pixels having approximately the same elevation. For steep slope areas, the fringe rate is high. Square windows, will cover more than one fringe. This will destroy the continuity of fringes and make phase unwrapping difficult. Consequently, directional windows should be used, such as the ones shown in Fig. 2. This makes filtering more effective in preserving the fringe pattern [3].

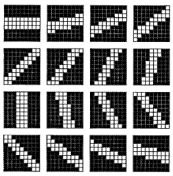

Figure 2: Sixteen directional masks for phase noise filtering. Only the white pixels are included in the computation.

For neighborhood structure GSM is used as a local description of the behavior of the cluster of coefficients centered at each coefficient in the pyramid. Since the neighborhoods overlap, each coefficient will be a member of many neighborhoods. The local model implicitly defines a Markov model, described by the conditional density of a coefficient in the cluster given its surrounding neighborhood, assuming conditional independence on the rest of the coefficients. In this paper, we simply use the estimation problem for the reference coefficient at the center of each neighborhood independently. To complete the interferogram model we need to specify the probability density, $p_z(z)$, and interferogram power spectral density (PSD).

4.3 Probability Density for Multiplier

Several authors have suggested the generalized Gaussian (stretched exponential) family of densities as an appropriate description of wavelet coefficient marginal densities [14, 15]: $p_x(x) \propto \exp(-|x/\alpha|^p)$, where the scaling variable controls the width of the distribution, and the exponent (p) controls the shape, and is typically estimated to lie in the range [0.5,0.8] for image subbands. Although these can be expressed as GSM's, the density of the associated multiplier has no closed form expression, and thus this solution is difficult to implement [16]. Others stated that the density of the log coefficient magnitude, log x, may be expressed as a convolution of the densities of (log u) and (log z). Since the density of (u) is known, this means that estimation of the density of may be framed as a deconvolution problem. The resulting estimated density may be approximated by a Gaussian, corresponding to a lognormal prior for the z. This solution has two drawbacks. First, it is only valid to the case when all the neighbors have the same marginal statistics, which, in practice requires they all belong to the same subband. Second, it is estimated from the noise-free coefficients, and it is difficult to extend it for use in the noisy case.

In this paper we use what is a so-called non-informative prior [16-17], which has the advantage that it does not require the fitting of any parameters to the noisy observation. Such solutions have been used in establishing marginal priors for image denoising [18]. In the context of estimating the multiplier from coefficients, this takes the form:

$$p_z(z)\alpha\sqrt{I(z)} \qquad I(z)=E\{-\frac{\partial^2 \log p(x|z)}{\partial z^2}\} \tag{11}$$

Where I(z) is the Fisher information matrix. Computing this for the GSM model is straightforward

$$-\frac{\partial^2 \log p(x|z)}{\partial z^2}=\frac{\partial^2}{\partial z^2}\left[\frac{1}{2}\left(N\log(z)+\log C_u+\frac{x^T C_u{}^{-1}x}{z}\right)\right] \tag{12}$$

$$= \quad \frac{N}{2z^2}+\frac{x^T{}_u{}^{-1}x}{2z^3}$$

taking the square root of the expectation, and using the fact that $E\left\{x^T C_u{}^{-1}x\right\}=z$ we obtain Jeffrey's prior which corresponds to a constant prior on log(z).

$$p_z(z)\alpha\frac{1}{z} \tag{13}$$

4.4 Interferogram PSD

The analysis presented in this section is based on the basic SAR interferometric system mode [19]. As shown in fig. 3, input to the system are the complex reflectivity functions $x_i(t)$, i = 1; 2. The impulse response functions are denoted with $h_{SAR;i}(t)$, i =1; 2. Each of these point target responses describes the individual end-to-end SAR imaging system. Finally, the interferogram Φ_z (t;τ) is formed from the focused SAR images $i_1(t;\tau)$ and $i_2(t;\tau)$. Her we introduce the variable t[s] to denote a time dimension (range or azimuth), and the extension to the two-dimensional domain is straightforward.

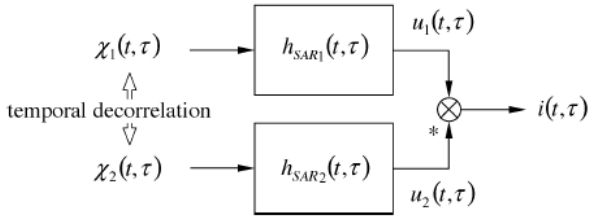

Figure 3: Interferometric system Model

The distributed scattered model constitutes the input to the interferometric system. The inputs $x_1(t)$ and $x_2(t)$ are correlated, unit variance complex, zero-mean Gaussian processes constructed from a(t), b(t), and c(t) which are of uncorrelated Gaussian type

$$x_1(t)=\sqrt{1-\gamma T}\,a(t)+\sqrt{\gamma T}\,c(t) \tag{14}$$

$$x_1(t)=(\sqrt{1-\gamma T}\,b(t)+\sqrt{\gamma T}\,c(t))\exp(-j2\pi\vartheta t)$$

a mutual correlation is realized by the factor γT (temporal coherence), and ϑ

$$S_{ii}=\frac{S_{u2u2}(f)\otimes S_{u1u1}(f)}{\int S_{u1u1}(f)df\int S_{u2u2}(f)df}\left|\gamma\vartheta\right|^2\delta(f-\vartheta) \tag{15}$$

denotes a fringe frequency attached to the second interferometric channel for ease of formulation. All parameter cases discussed in the following section are based on

subsequently derived formulation of the interferogram PSD function. For transfer functions with finite bandwidth (which is true for any real SAR system), the interferometric PSD is easily calculated as the Fourier transform of the interferogram sample autocorrelation function (ACF) [20].

Equation (15) represents the normalized interferogram PSD so as to emphasize that the square of the coherence determines the line mass of its right-hand-side second term ($\otimes$ denotes cross correlation).

$S_{I1\ I1}$ (f) and $S_{I2\ I2}$ (f) denote the PSDs of the SAR images, and δ(.) denotes the Dirac Delta Distribution. As can be shown, the fringe frequency is found as frequency shift in the argument of the Delta function. From the definition of the interferogram ACF (Holzner 2002), it is clear that no phase bias can be measured neither from the interferogram ACF nor from the interferogram PSD. As described by [10], the individual terms of the PSD are defined as:

$$S(f) = P_S(f) + m\,\delta(f) \tag{16}$$

The first term of the PSD is referred to as pedestal $P_S(f)$ with an integral value of 1 (due to the normalization of the power spectrum), and m refers to the spectral line mass.

5. INTERFEROGRAM FILTERING

Recognizing the residuals sensitivity of 2-D phase unwrapping algorithms, it would be useful to reduce the residuals from the measured interferogram before processing them further. The main concern in the proposed scheme is not to affect the fringes (line of discontinuity) with respect to their location, sharpness, and jumps of height. Other requirements are low computational complexity, robustness, and ease of use.

Our filter procedures use the top-level structure as most previously published approaches and can be summarize as follows:

1) Decompose the interferogram into pyramid subbands at different scales and orientations;
2) Apply the filter at each subband, except for the low pass band.
3) Invert the pyramid transform, obtaining the denoised image.

The assumption that the residuals are exhibits a white Gaussian with known variance [3] is used in this paper. A vector y corresponding to a neighborhood of N observed coefficients of the pyramid representation can be expressed as

$$y = x + w = \sqrt{z}u + w \tag{17}$$

Based on GSM structure of N Coefficients, and the assumption that the residuals act as independent additive Gaussian. The parameters u, w, and z are independent. both u and w are zero-mean Gaussian vector [19], with associative covariance C_u and C_w. the density of the observed neighborhood vector conditioned on z is a zero-mean Gaussian, with covariance $C_{y|z} = zC_u + C_w$. The neighborhood noise covariance, C_w, is obtained by decomposing a function $\sigma\sqrt{N_y N_x PSD_r(i)}$ into pyramid subbands, where N_x ,N_y are the interferogram dimensions, and $PSD_r(i)$ is the inverse Fourier transform of the square root of the interferogram power spectral density. This signal has the same power spectrum as the residual, but it is free from random fluctuations. Elements of C_w may then be computed directly as sample covariance (i.e., by averaging the products of pairs of coefficients over all the neighborhoods of the subband). Given C_w, the signal covariance C_u can be computed from the observation covariance matrix. C_y is computed from $C_{y|z}$ by taking expectations over z: taking an assumption that E{z} = 1.

$$C_y = E\{z\}C_u + C_w \tag{18}$$

5.1 Bayes Least Square Estimation

For each neighborhood, we wish to estimate x_c, the reference coefficient at the center of the neighborhood, from y, the set of observed coefficients. The Bayes least squares (BLS) estimate is just the conditional mean.

$$\begin{aligned} E\{x_c\, y\} &= \int x_c\, p(x_c|y)dx_c \\ &= \int_0^{\infty}\int x_c\, p(x_c, z|y)dzdx_c \\ &= \int_0^{\infty}\int x_c\, p(x_c\, y, z)p(z, y)dzdx_c \\ &= \int p(z, y)E\{x_c|y, z\}dz \end{aligned} \tag{19}$$

Thus, the solution is the average of the Bayes least squares estimate of x when conditioned on z, weighted by the posterior density, p(z|y) .We now describe each of these individual components.

According to GSM model, the neighborhood coefficients of vector x is Gaussian when conditioned on z. Coupled with the assumption that the residuals are characterized as Gaussian noise. This means that the expected value inside the integral 8 is local linear (Wiener) estimate. Writing this for the full neighborhood vector

$$E\{x|y, z\} = zc_u(zC_u + C_w)^{-1}\, y \tag{20}$$

Portellia et. al, simplified this expression [10] result in:

$$E\{x_c\, y, z\} = \sum_1^N \frac{zm_{cn}\lambda_n v_n}{z\lambda_n + 1} \tag{21}$$

where $m_{i,j}$ represents an element (i-th row, j-th column) of the matrix M , s is the symmetric square root of the positive definite matrix c_w and A is the eigenvalue expansion of the matrix $S^{-1}C_uS^{-T}$, λ_n are the diagonal elements of A, v_n is the elements of $v = M^{-1}$ y , and c is the index of the reference coefficient within the neighborhood vector, which considered a first part of eq. (8). The other component of the solution given in (8) is the distribution of the multiplier, conditioned on the observed neighborhood values. We use Bayes' rule to compute this

$$p(z|y) = \frac{p(yz)p_z(z)}{\int_0^{\infty} p(y\alpha)p_z(\alpha)d\alpha} \tag{22}$$

we choose a non-informative Jeffrey's prior, corrected at the origin, for the function $p_z(z)$. The conditional density p(y|z) is given in eq. (6), and its computation may be simplified using the relationship in eq. (10) and the definition of v

$$p(y|z) = \frac{\exp(-\frac{1}{2}\sum_{n=1}^{N}\frac{v_n^2}{z\lambda_n + 1}}{\sqrt{(2\pi)^N |C_w \prod_{n=1}^{N}(z\lambda_n + 1)}} \tag{23}$$

5.2 Filtering Process

According to the proposed scheme and [16], Filtering interferogram process can be summarized as follows:

1) Decompose the interferogram into subbands.
2) For each subband (except the low-pass):
    a) Compute neighborhood noise covariance from the image-domain noise covariance.
    b) Estimate noisy neighborhood covariance.
    c) Estimate C_u from C_w and C_y using eq. (18).
    d) For each neighborhood:
        i) For each value z in the integration range:
            A) Compute $E\{x_c y, z\}$ using eq. (21).
            B) Compute $p(y|z)$ using eq. (23).
        ii) Compute $p(z|y)$ using eqs. (22) and (13).
        iii) Compute $E\{x_c y\}$ numerically using eq. (19).
3) Reconstruct the denoised image from the processed subbands and the lowpass band.

6. EXPERIMENTAL RESULTS

The proposed scheme for interferogram filtering is applied to real interferometric SAR (InSAR) image. The size of the image in pixels is 512 (azimuth) × 512 (range). The estimated surfaces are compared with the reference digital Elevation Model (DEM). Figure 4-a) shows the phase image of original interferogram while figure 4-b) shows the reference DEM. In the available literature on interferogram filtering, the method of choice is often judged by visually comparing original and processed interferogram. In addition to visual judgment, quantitative evaluations are used during this work includes:

a) Peak Signal to Noise Ratio (PSNR) between filtered and original phase.
b) Reduction of the residuals counts.
c) Quantitative effect on phase unwrapping.

In order to evaluate the effect of complex interferogram filtering on 2-D phase unwrapping quantitatively, we consider determination of the phase field estimation by means of Goldstein algorithm [1].The unwrapped phase values are compared with the reference data shown in figure 4(b). Three other filtering algorithms are used for evaluation, they are: pivoting median filter [1]. With 3X3 window size, 2) max-flat filter defined in [1] and modified Goldstein filter [21].

In general, it can be stated that the Peak Signal to Noise Ratio (PSNR) for proposed scheme reaches 45 db. Moreover the number of residuals after filtering process decreased by 78.6%. Table 1 summarizes the PSNR and residual counts for different techniques

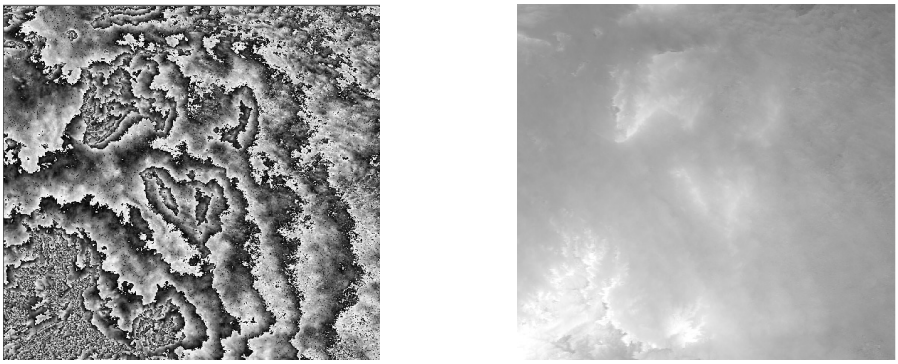

(a) (b)

Figure 4: Demonstrate the Input Phase Images a) Original Unwrapped Phase. b) Reference Wrapped Phase.

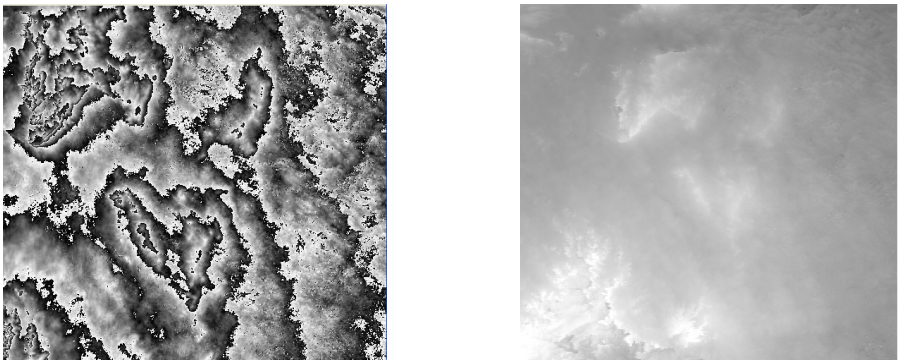

(a) (b)

Figure 5: Demonstrate the output Images a) filtered Unwrapped Phase. b) Wrapped Phase.

Another evaluation parameter applied to the complex interferogram filtering is subsequent phase unwrapping including height inversion (DEM). This is done by taking the interferogram with and without preprocessing as input to Goldstein algorithm [1]. Table 2 lists the average errors between wrapped phase with and without preprocessing and the original height values. It is verified that the proposed scheme introduces the best average error, affecting directly the accuracy of terrain height.

	Original Interferogram	Proposed	Max-flat	Pivoting Median	Modified Goldstein
PSNR (dB)		45	11.6	15.7	38
Number of Residues	13785	2956	12306	1843	3456

Table 1: Performance Evaluation Measures

	DEM without filtering	DEM after proposed filtering	DEM after Max-flat	DEM after Pivoting Median	Modified Goldstein
Average error(Meter)	63.1	12.3	42.3	97.6	18

Table 2: Average Error of Height Inversion of Input Interferogram using Different Filters

Qualitative measures of the output phase data, as shown in figure (3), indicate the superiority of the proposed scheme. It demonstrates good adaptively of proposed scheme as it reduces the residues count while preserving edges and fine details. The pivoting median filter gives good results of residues reduction but introduces smoothness at level of phase details. Max-flat filter is better than pivoting median filter. The output wrapped phase data is shown in figures (6), while figures (7,8) shows the 3d and close look images for better evaluation process.

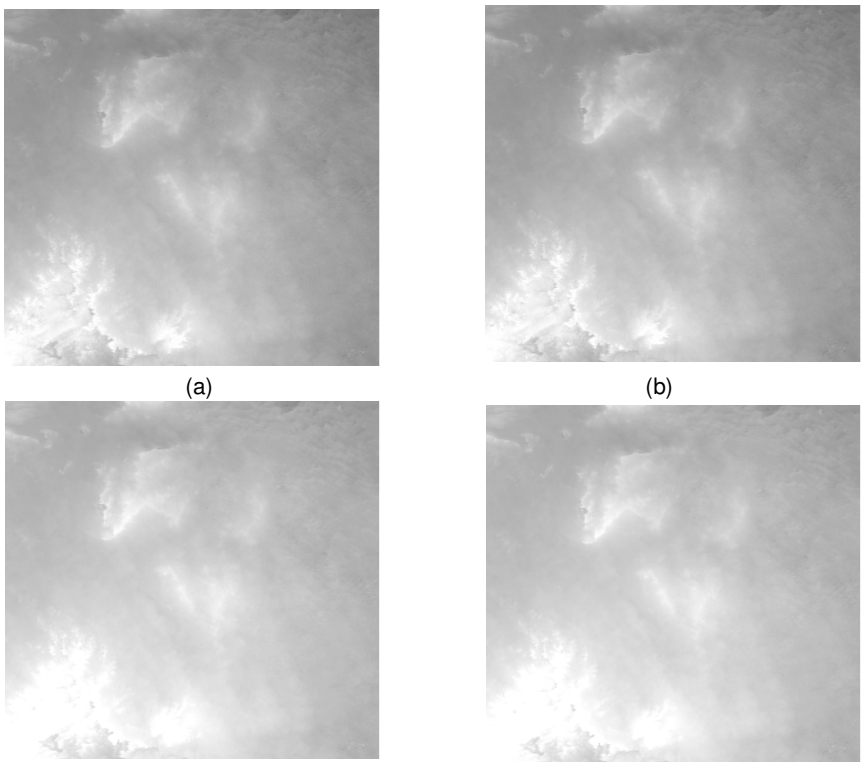

Figure 6: Output Unwrapped Phase Data after Different Filtering Process
a) proposed b) Max-Flat c) Pivoting Median d) Modified Goldstein

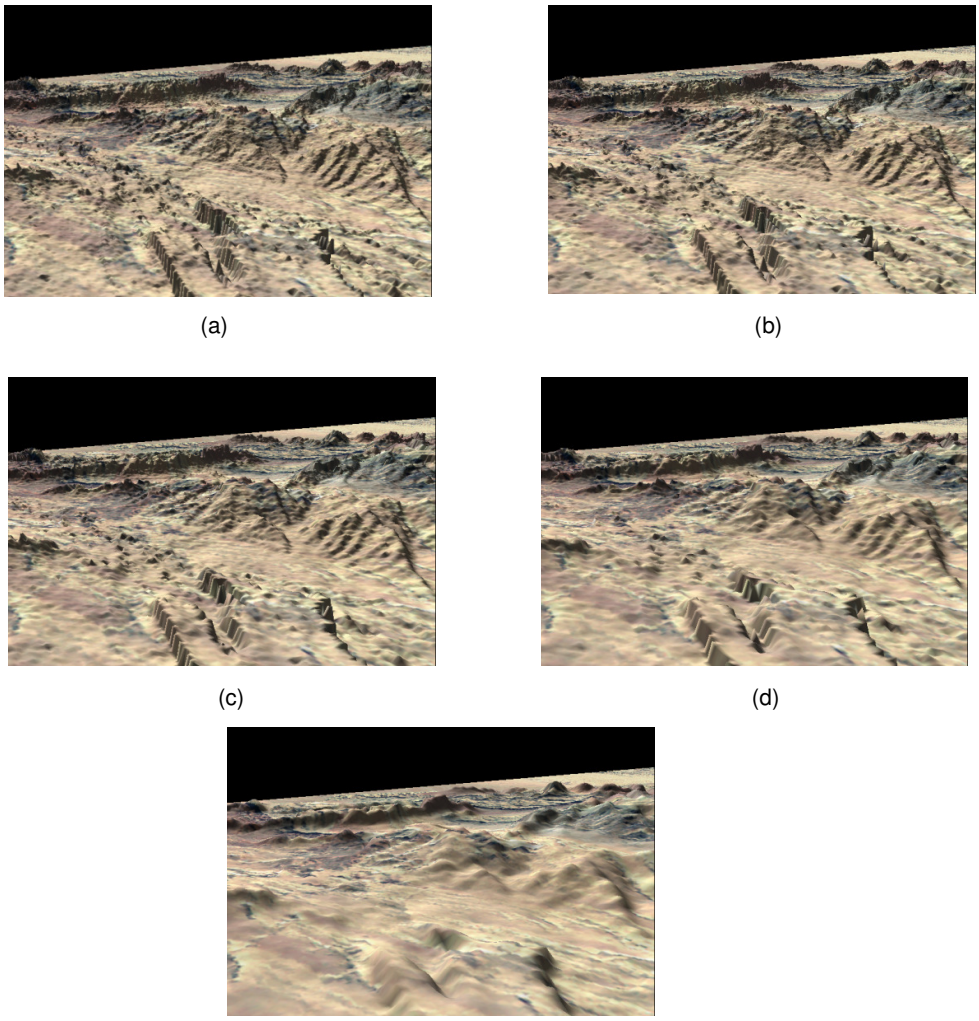

(a) (b)

(c) (d)

(e)

Figure 7: Perspective Phase Unwrapped Images a) Reference DEM b) proposed filter c) modified Goldstein d) Max-Flat e) Median filter

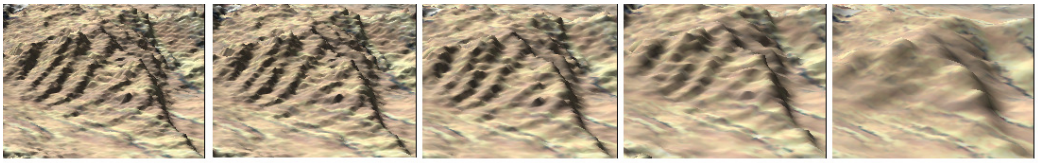

(a) (b) (c) (d) (e)

Figure 8: Closer Look of Perspective Phase Unwrapped Images a) Reference DEM b) proposed filter c) modified Goldstein d) Max-Flat e) Median filter

CONCLUSIONS

To obtain a more accurate unwrapped phase, a new scheme has been proposed based on a local Gaussian scale mixture model for reduction residual counts in interferogram. The approach uses Steerable wavelet decomposition. At each scale, a noise covariance matrix is estimated for the neighborhood of each pixel using interferogram power spectral density. The covariance is then used to produce a maximum a-posteriori estimate of the noise-free value of the pixel. After the image has been de-noised at each scale-level, it is then reconstructed.

Comparing with other interferogram filtering, the proposed scheme achieves 78.6% in reduction of residual count. On the other hand Max-Flat, Pivoting Median , and modified Goldstein has also the ability to reduce the residues count by 10.7%, 86.7 % and by 74.9 respectively.

Comparing the unwrapped phase with reference DEM, median filter achieves higher average error followed by Max-flat, modified goldestien and the proposed method comes with the lowest average error. The results of the unwrapped phase image show that the proposed scheme has the ability to reduce the residues count while preserving the phase discontinuity.

It has been proved that lowering residues count does not guarantee high unwrapping accuracy; since the median filter has the ability to reduce the residual count by 86.7% meanwhile introduces the worst DEM accuracy with 97.7 meter as an average error.

REFERENCES

[1] Ghiglia, D.C. and Pritt, M. D. “Two-Dimensional Phase Unwrapping: Theory, Algorithms, and Software”. New York: Wiley 1998.

[2] López, C.M., Eric, P."Coherence estimation in synthetic aperture radar data based on speckle noise modeling.". Applied Optics, 46(4):544-558, 2007

[3] Lee, J. S., Papathanassiou, K. P., Ainsworth, Grunes, T. L., M. R, Reigber, A. "A new technique for noise filtering of SAR interferometric phase images". *IEEE* Transactions on Geoscience and Remote Sensing, 36(5):1456–1465, 1998

[4] Chang, Ge. L. and Rizos, C. "Mine subsidence monitoring using multi-source satellite SAR images”. Photogrammetric Engineering and Remote Sensing, 73(3):259-266, 2007

[5] Ferraiuolo, G. and Poggi, G. "A Bayesian filtering technique for SAR interferometric phase fields". IEEE Transactions on Image Processing, 13(10):1368 – 1378, 2004

[6] Andrews, A. F. and Mallows, C. "Scale mixtures of normal distributions". Journal of the Royal Statistical Society. Series B, 36(1), 99-102, 1974

[7] Guarnieri, A. M. "SAR interferometry and statistical topography". IEEE Trans. Geoscience and Remote Sensing, 40(12): 2567–2581, 2002.

[8] Kingsbury, N. G. "Image processing with complex wavelets". Philosophical Transactions: Mathematical, Physical and Engineering Sciences Royal Society London, 357 (1760):2543-2560, 1999

[9] Kingsbury, N. G. "Complex wavelets for shift invariant analysis and filtering of signals". Journal of Applied and Computational Harmonic Analysis, 10(3): 234-253, 2001

[10] Portilla, J, Simoncelli, E P. "A Parametric Texture Model based on Joint Statistics of Complex Wavelet Coefficients". Int. Journal of Computer Vision, 40(1):49-71, 2000

[11] Liu, J., Moulin, P. "Complexity-Regularized Image Denoising". IEEE Transaction on Image Processing,10(6):841-851, 2001

[12] Starck, J .L., Candes, E. J., Donoho, D. L. "The curvelet transform for image denoising". IEEE Transaction on Image Processing, 11(6):670–684, 2002

[13] Simoncelli, E. P., Freeman. T., Adelson, E. H., Heeger, D. J. "Shiftable multi-scale transforms". IEEE Transaction on Information Theory, 38(2):587–607, 1992

[14] Simoncelli, E. P. and Adelson, E. H. "Noise removal via Bayesian wavelet coring". Proceedings of 3rd IEEE International Conference on Image Processing, 1996

[15] Moulin, P., Liu, J."Analysis of multiresolution image denoising schemes using a generalized Gaussian and complexity priors". *IEEE Transaction on Information Theory*, 45(3): 909–919, 1999

[16] Portilla, J., Strela, V., Martin J., Simoncelli, E. P. "Denoising Using Scale Mixtures of Gaussians in the Wavelet Domain". IEEE transactions on image processing,12(11):1338-1350, 2003

[17] Box, G. and Tiao, C. “Bayesian Inference in Statistical Analysis”. New York: Addison-Wesley, 1992.

[18] Figueiredo , M., Nowak, R. "Wavelet-based image estimation: An empirical Bayes approach using Jeffrey’s noninformative prior". *IEEE Transaction on Image Processing*, 10(9):1322–1331, 2001

[19] Holzner,J. "Analysis and Statistical Characterization of Interferometric SAR Signals Based on the Power Spectral Density Function". IEEE transactions on geoscience and remote sensing, 42(5):1116-1121, 2004

[20] Holzner, J., Bamler, R., "Burst-mode and ScanSAR interferometry”. IEEE Transaction on Geoscience and Remote Sensing, 40(9):1917–1934, 2002

[21] Li, Z.W., Ding, X.L. Huang, C. Zhu, J.J., Chen, Y.L. "Improved filtering parameter determination for the Goldstein radar interferogram filter". International Society for Photogrammetry and Remote Sensing, Inc. (ISPRS), 63(6):621-634, 2008